Software-Defined Distributed SIMO System for Underwater Communication

Kerem Enhos, Deniz Unal, Emrecan Demirors and Tommaso Melodia
Institute for The Wireless Internet of Things, Northeastern University, Boston, MA, USA
Email: {enhos.k, unal.d, e.demirors, melodia}@northeastern.edu

***Abstract*—Wide-ranging applications for underwater acoustic communication are attracting attention. However, the challenges of underwater acoustic communications make it necessary to advance communication techniques significantly. Underwater networks with wider coverage areas and more reliable communication links may be possible with the distributed deployment of several reception nodes. Using Single Input Multiple Output (SIMO) systems, power, and bandwidth resources can be utilized effectively without compromising spectral efficiency. In this work, we propose a communication system that employs software-defined distributed SIMO networking to exploit the spatial diversity of multiple receiver nodes for high data rates and reliable communication. To take advantage of spatial diversity, we develop and implement a software-defined architecture for the maximal-ratio combining receiver. Then, we conduct a thorough experimental evaluation in ocean environments for various subcarrier bandwidths and constellations using three distributed receivers. Our results show that our proposed distributed SIMO system, for both 1x2 and 1x3 settings, outperforms individual receiver modems in terms of bit error rate (BER) performance by 95.20% and 99.57%, respectively.**

***Index Terms*—Underwater Acoustic Communication, Distributed MIMO, Maximal-ratio Combining, Software-Defined Modem.**

I. Introduction

Underwater acoustic communication has a wide range of applications for commercial and military activities incorporating underwater vehicles and sensor networks that can collaboratively accomplish tasks. For autonomous operations of these nodes, efficient and robust communication links are vital. However, inherent challenges of underwater acoustic communications such as Doppler spreading, severe multipath, high path loss, delay spread, and limited bandwidth create the need for significant improvements over communication methods [1].

One of the techniques that can enhance the quality of underwater acoustic communication links is diversity combination with multiple receivers, often denoted as single-input multiple-output (SIMO). With this technique, channel capacity can be increased, and utilization of power and bandwidth resources can be enabled efficiently without decreasing the spectral efficiency [2]. Although for conventional SIMO systems, receiving antennas are co-located, for underwater systems, spatial diversity can also be exploited by the distributed deployment of several single antenna receiver nodes over vast ocean areas. Such distributed SIMO clusters generated through cooperation between geographically separated antenna receivers can pave the way for high data rate underwater networks with wide coverage areas.

Acknowledgement: This work was supported by the National Science Foundation under Grant CNS-1763964 and Grant CNS-1726512.

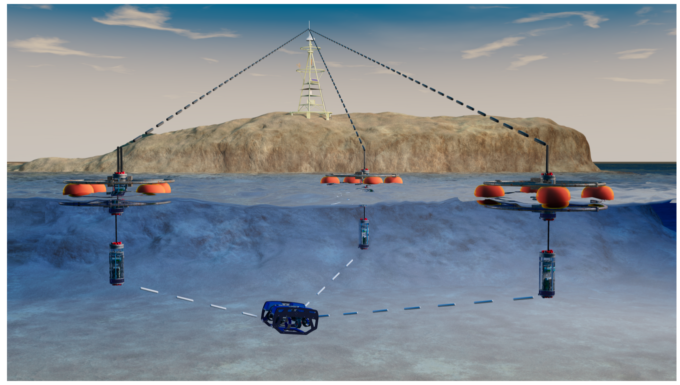

Fig. 1. Software-defined distributed SIMO systems can be used to retrieve information from a mobile transmitter node (e.g., UUV).

Figure 1 depicts a sample use case scenario where a distributed SIMO system can be used to retrieve information from a mobile transmitter node (e.g., unmanned underwater vehicle (UUV)) hovering and performing tasks within a coverage area of multiple receivers. By exploiting the spatial diversity generated with the distributed SIMO system, the mobile transmitter node can obtain higher channel capacity and accordingly higher data rates without leveraging more power and bandwidth resources or limiting communication ranges. As shown in Fig. 1, pre-processing of the received signals can be implemented on the software-defined underwater modems [3], [4], then necessary information can be transferred to remote cloud servers with the help of smart buoys [5] for time synchronization and further processing of diversity combining. With this extendable system, by increasing the number of receivers, wider coverage areas can be utilized, and communication performance can be improved.

In addition to improving the channel capacity and coverage area, distributed SIMO systems can be beneficial for scenarios where high interference, fading, or blockage is present in the communication channel. Instead of relying on one communication link, the collaborative operation of such SIMO systems can prevent interruption for mobile communication nodes and enables robust communication links. With the software-defined architecture, the operation of these distributed modems can be reconfigured and optimized in a cellular network manner. Depending on the channel conditions, modems can be instructed to operate for a different task or assigned to collaborate in the SIMO system for an improved communication link.

978-1-5386-7462-8/23/$31.00 ©2023 IEEE

Previously, multiple-input multiple-output (MIMO) techniques are discussed for underwater acoustic communications using orthogonal frequency division multiplexing (OFDM) [6]–[8] with both using simulated and experimental data. However, these works only consider the co-located antenna systems and neglect the evaluation of the distributed deployment of underwater communication nodes. In [9], distributed deployment of a multiple-input single-output (MISO) system is discussed. The system, including two transmitters with a 15 ft separation and a receiver modem located at a distance of 450 ft from the transmitters, are assessed through lake experiments.

In this work, we propose a communication system that *enables high data rate and robust communication by exploiting the spatial diversity of multiple receiver nodes using software-defined distributed SIMO networking*. The proposed system incorporates multiple individual receivers that can receive the transmitted signals from a single transmitter. Then the received signals are pre-processed on the software-defined modems in an edge computing manner, which are then transferred to cloud servers for further processing through smart buoy gateways.

In this paper, we design and implement the software-defined architecture for maximal-ratio combining receiver to exploit the spatial diversity in Section II. Then in Section III, extensive experimental evaluation is conducted in Boston Harbor, MA, USA, for different subcarrier bandwidths and constellations over different signal-to-noise ratio levels by using three distributedly deployed receivers. Numerical results are obtained, and comparisons are presented for individual receivers, 1x2 and 1x3 SIMO systems. Concluding remarks are given in Section IV.

II. System Model

The evaluation of the MRC for distributed SIMO systems is realized by using the software-defined underwater acoustic networking platform, the SEANet modem [3], [4]. For detailed hardware implementation, readers can refer to [10]. By exploiting the software-defined networking capability of the SEANet modem, custom ZP-OFDM waveforms are generated and transmitted.

In the experiments conducted in Section III, four different ZP-OFDM physical layer settings are investigated. For each setting utilized bandwidth is kept constant. Firstly, subcarrier bandwidths are differentiated. In the first setting, subcarrier bandwidth of 7.63 Hz is used where 8192 subcarriers are used over 62.5 kHz total bandwidth. For the second setting, subcarrier bandwidth is increased to 15.26 Hz. In this setting 125 kHz of total bandwidth is utilized by 8192 subcarriers, however, only 4096 subcarriers are used for data transmission and the rest of the subcarriers are assigned as null subcarriers. In the first two settings, symbols are mapped over binary phase shift keying (BPSK) constellation points. For the third and fourth settings, two different subcarrier bandwidths are investigated again with quadrature phase shift keying (QPSK) constellation points. Although utilized bandwidth is kept constant at 62.5 kHz, data rates are increased by using QPSK symbol mapping for the last two settings.

These different ZP-OFDM waveforms are generated in baseband, which then upconverted and transmitted at $150\,\text{kHz}$ center frequency with a custom projector transducer that has resonance frequency at $145\,\text{kHz}$. Similarly, after the reception with an omnidirectional hydrophone (Teledyne TC4013) implemented on the receiver modems, downconversion is applied in order to process the received signals in the baseband.

Each ZP-OFDM packet consists of linear frequency modulated (LFM) up-chirp and pseudo-noise (PN) sequences as preambles, OFDM packet, LFM down-chirp as postamble, and zero-padding between each component. LFM up-chirp and down-chirp are used for Doppler estimation and compensation of each ZP-OFDM packet. After successful Doppler compensation, OFDM symbol detection is performed by cross-correlation of the PN sequence. After demultiplexing the OFDM symbol, carrier frequency offset (CFO) estimation and compensation are performed by bounded minimization function utilized by minimizing the energy levels of known null subcarriers [9]. Thus, the received OFDM symbol can be expressed as

$$y = h \cdot x + n, \tag{1}$$

where x is the transmitted signal, h is the channel response, n is the noise received at the receiver, and y is the resulting received signal. With the usage of pilot subcarriers known to the receiver, channel response can be estimated and with equalization of the channel component the transmitted signal can be estimated by using zero-forcing equalizer as [11]

$$\hat{y} = (h^* h)^{-1} h^* y. \tag{2}$$

Thus, OFDM symbol equalization can be implemented for each individual receiver. For communication systems where multiple receiver antennas are utilized, Eq. (1) can be rewritten as [12]

$$\begin{bmatrix} y_1 \\ y_2 \\ \vdots \\ y_N \end{bmatrix} = \begin{bmatrix} h_1 \\ h_2 \\ \vdots \\ h_N \end{bmatrix} \cdot x + \begin{bmatrix} n_1 \\ n_2 \\ \vdots \\ n_N \end{bmatrix}. \tag{3}$$

For SIMO systems, where multiple receivers are utilizable, maximal-ratio combining (MRC) can be applied to the received signals. With MRC, output SNR can be maximized by weighing the received signals that propagated through different channel responses for each receiver, and then combining the weighted signals [13]. Hence, by using MRC, the resulting weighted received signal can be obtained by rewriting Eq. (2) with considering Eq. (3) [12], [14]

$$\hat{y}_{MRC} = \frac{h_1^* y_1 + h_2^* y_2 + ... + h_N^* y_N}{|h_1|^2 + |h_2|^2 + ... + |h_N|^2} \tag{4}$$

where N denotes the number of receiver antennas. By using this MRC algorithm, received signals from deployed receiver modems in a distributed manner are firstly processed to estimate each individual channel, then the channel estimations are used to weight and combine the signals in order to obtain maximum-ratio combined waveform, $\hat{y}_{MRC}$, which SNR is maximized according to the relative communication channels.

Implementation of this system is enabled by the software-defined architecture of the SEANet modems. Custom generated waveforms are transmitted from a modem and received from three different modems simultaneously. Each receiver's received signals are then streamed to a remote server for further signal processing. The signal processing chain starts with packet detection and synchronization. Each packet is detected by using LFM preambles and packets are synchronized at the remote server to be further processed as explained previously. An overall block diagram is given in Fig. 2. Each receiver independently performs Doppler and CFO estimation/compensation and channel estimation, then the estimated channel responses are weighted and combined with MRC.

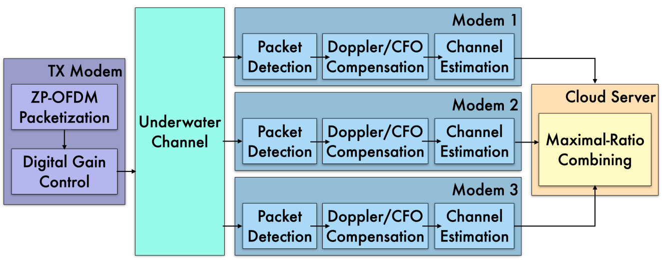

Fig. 2. Block diagram for the distributed SIMO system with MRC.

III. Experimental Results

In this section, experimental evaluation of the software-defined distributed SIMO system is conducted for underwater communication. Experiments are conducted in Charlestown Marina, MA, USA with a semi-permanent testbed. Four software-defined underwater acoustic modems, which are described in Section II, are deployed through the docks by securing them to the dock cleats. The transmitter modem is deployed at $1\,\mathrm{meter}$ depth using a transducer that has $-3\,\mathrm{dB}$ beamwidth of 60° with hemispherical beam pattern. Hence, in order to have efficient transmission, the transmitter modem is deployed facing toward the ocean bottom. Three receiver modems are deployed at $12\,\mathrm{meters}$ depth facing towards to ocean surface with $0.5\,\mathrm{meter}$ separation between each other. With this deployment setup, each transmitter-receiver connection maintains a vertical communication channel, which is important for minimizing the multipath effect.

All the modems are connected to individual gateway buoys that enable LTE connection to each modem. With this capability, desired data or waveforms can be streamed or recorded through the underwater modems. In addition to data access, received waveforms can be streamed to a remote server for computationally intensive operations in a cloud computing manner. For all the experiments conducted in this section, received signals by the underwater modems are streamed to a remote server, where cloud computation of MRC, channel equalization, and demodulation operations are implemented.

Generated waveforms described in Section II, different physical layer settings are transmitted through the transmitter modem and received from each receiver modem simultaneously for each waveform. Received signals are streamed to the cloud computing server and the MRC algorithm is applied for considering all three receiver modems (1x3 SIMO system) and for each pair of receivers (1x2 SIMO system) separately. Since each receiver modem is deployed in a distributed manner, channel responses for each receiver are substantially different from each other as shown in Fig. 3, which causes differentiation in communication performance of each receiver pair, if MRC algorithm is applied in a 1x2 SIMO setting. Thus, bit-error-rate (BER) performance over different signal-to-noise ratio (SNR) levels are shown individually for 1x2 and 1x3 SIMO settings. During the experiments, SNR level is differentiated by changing the gain of the transmitter. Assuming that the noise level is constant, the signal level is lowered for lower SNR levels.

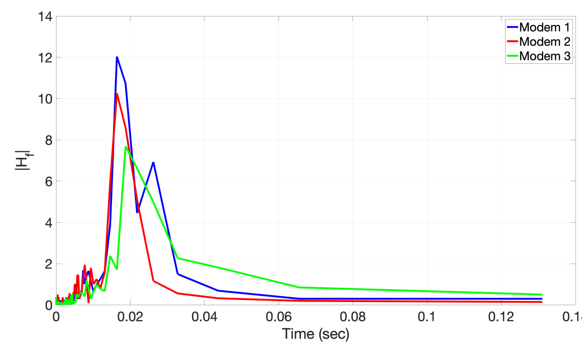

Fig. 3. Impulse response of individual receiver modems are given. Each modem's communication channel has a distinct response.

A. 1x2 SIMO

Firstly, for each physical layer setting, MRC algorithm is applied for SIMO systems where only two receivers are utilized. Since three distributed receiver modems are deployed, each pair results in different BER performance due to the substantial difference between each channel.

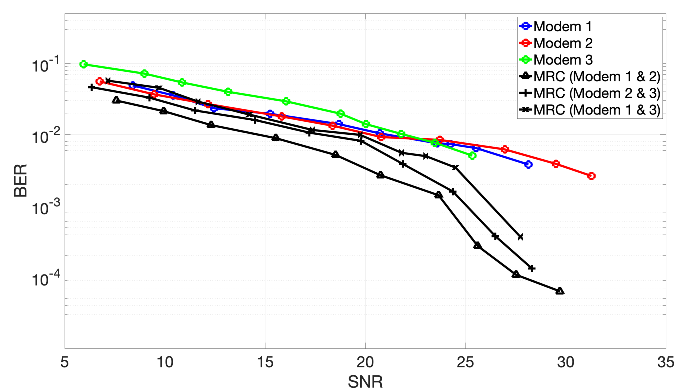

Fig. 4. BER results for 1x2 SIMO system with 15.26 Hz subcarrier bandwidth and BPSK constellation is given for each receiver pair. BER results of each individual receiver is also shown.

As shown in Fig. 4 and Fig. 5, BER performance is improved with the MRC algorithm at higher SNR levels.

Although *Modem 1* and *Modem 2* pair performs better compared to other receiver pairs, substantial improvement can be observed for every pair. For such distributed systems, every channel has different impulse responses, which may result in performance differentiation for each 1x2 SIMO pairs.

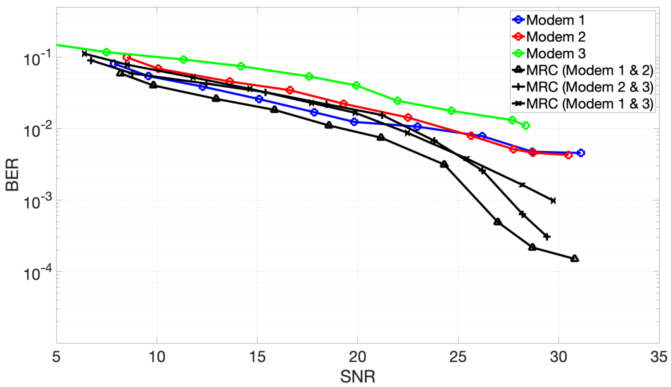

Fig. 5. BER results for 1x2 SIMO system with 7.63 Hz subcarrier bandwidth and BPSK constellation is given for each receiver pair. BER results of each individual receiver is also shown.

After observing the results for BPSK symbol mapping, two waveforms with different subcarrier bandwidths are analyzed for QPSK constellation. Although the data rate is increased with this symbol mapping, BER performance is worse compared to BPSK. However, similarly to the BPSK setting, MRC algorithm improves the BER performance for each 1x2 SIMO pair. It can be seen that in Fig. 6, BER performance is worse at low SNR levels for *Modem 1* and *Modem 3* pair, although BER performance of *Modem 1* is better as an individual receiver source. This is due to the high channel impairment in *Modem 3*. As explained previously, substantial channel impulse response differentiation for individual modems can lead to underperformed SIMO systems.

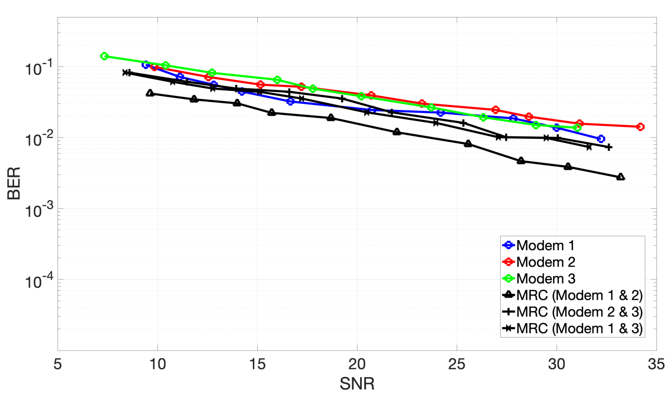

Fig. 6. BER results for 1x2 SIMO system with 15.26 Hz subcarrier bandwidth and QPSK constellation is given for each receiver pair. BER results of each individual receiver is also shown.

For Fig. 7, although MRC algorithm performs better in terms of BER for each pair compared to individual receiver modems, performance improvement is more significant for communication links that have high SNR. Although BER performance for individual receiver modems are similar, the deviation between the channel responses can lead to BER performance differentiation for different receiver pairs. As shown in Fig. 7, 87.56% BER performance improvement can be obtained for different receiver pairs at the same SNR level.

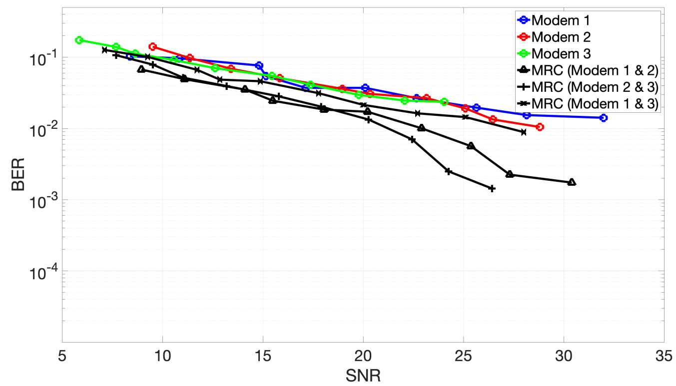

Fig. 7. BER results for 1x2 SIMO system with 7.63 Hz subcarrier bandwidth and QPSK constellation is given for each receiver pair. BER results of each individual receiver is also shown.

B. 1x3 SIMO

The same received data that is used for Section III-A is used to investigate the MRC algorithm for 1x3 SIMO systems by using three individual receiver modems that are deployed in a distributed manner.

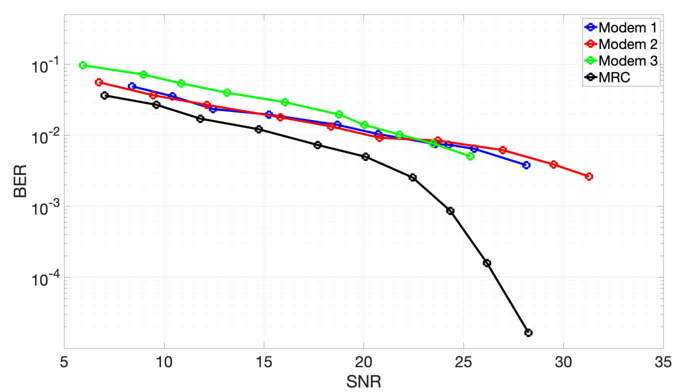

Fig. 8. BER results for 1x3 SIMO system with 15.26 Hz subcarrier bandwidth and BPSK constellation is given. BER results of each individual receiver is also shown.

Firstly, BPSK constellation is observed with different subcarrier bandwidths as shown in Fig. 8 and Fig. 9. Compared to 1x2 SIMO systems, MRC algorithm with three individual receivers outperforms in terms of BER for all SNR levels. Performance improvement increases at higher SNR levels due to more accurate channel estimation.

For different subcarrier bandwidths, BER results for individual receiver modems and 1x3 distributed SIMO system are shown in Fig. 10 and Fig. 11. Using QPSK symbol mapping decreases the BER performance at same SNR levels compared to BPSK. However, performance improvement of MRC algorithm is more significant compared to 1x2 SIMO systems.

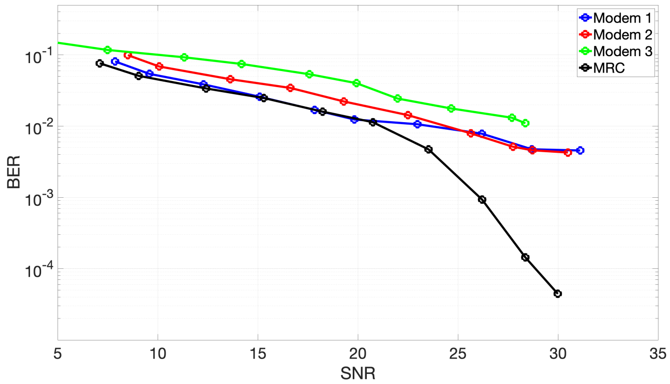

Fig. 9. BER results for 1x3 SIMO system with 7.63 Hz subcarrier bandwidth and BPSK constellation is given. BER results of each individual receiver is also shown.

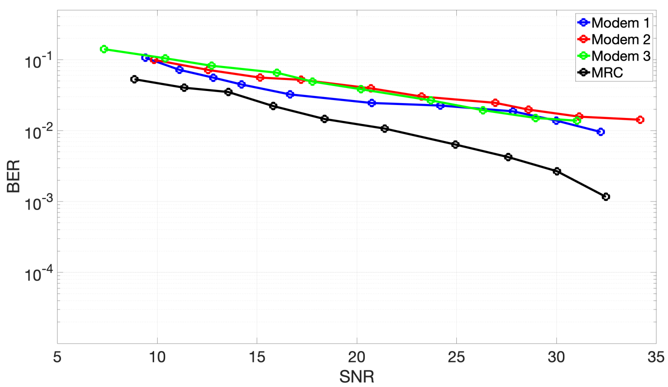

Fig. 10. BER results for 1x3 SIMO system with 15.26 Hz subcarrier bandwidth and QPSK constellation is given. BER results of each individual receiver is also shown.

After assessing the BER results for different subcarrier bandwidths, it is shown that the communication performance is similar at the same SNR levels for each different setting. However, channel impairment and response of each distributed receiver modem are exceedingly important for the performance of MRC algorithm. For significantly differentiated channels, MRC algorithm performs worse. Also, accurate channel estimation is vital for MRC algorithm. At high SNR levels, channel estimation is more accurate which leads to greater improvement in MRC performance.

Though for every setting, it is shown that MRC algorithm improves the BER performance and increasing the number of receivers also lead to significant improvement for each setting. In Fig. 13 (left), constellation diagrams for the received bits are shown for each individual receiver modem. Spreading of bits over in-phase and quadrature axis deteriorates the demodulation performance. However, after the MRC algorithm is applied for three different channels, error vector magnitude (EVM) decreases at the same SNR level, as shown in Fig. 13 (right).

BER result for each packet is obtained and for packets that don't have any errors, BER is denoted as 1×10^{-4}, which is approximately the lowest BER that can be obtained with the given data size of the generated ZP-OFDM packets. Though, for individual receivers BER performance are similar, MRC

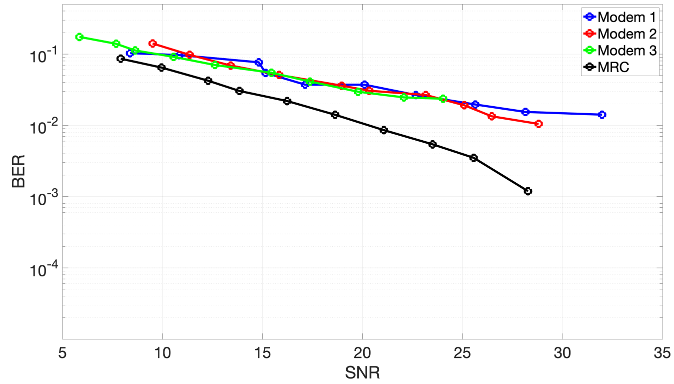

Fig. 11. BER results for 1x3 SIMO system with 7.63 Hz subcarrier bandwidth and QPSK constellation is given. BER results of each individual receiver is also shown.

improves the BER performance for each packet, as shown in Fig. 14.

In Fig. 12, BER results for individual receivers, receiver pairs of 1x2 SIMO system and 1x3 SIMO system are given for different subcarrier bandwidths and modulation orders at the same SNR level of 30dB. BER improvement can be visualized more adequately with this figure.

TABLE I

NUMERICAL REPRESENTATION OF AVERAGE BER RESULTS AND PERCENTAGE IMPROVEMENT OF BER IN DB SCALE WITH MRC ALGORITHM FOR 1X2 AND 1X3 SIMO SYSTEMS COMPARED TO INDIVIDUAL RECEIVERS (1X1).

Setting	Result	1x1	1x2	1x3
1	BER	0.00384	1.88×10^{-4}	1.66×10^{-5}
	%	-	95.20	99.57
2	BER	0.0125	5.82×10^{-3}	1.16×10^{-3}
	%	-	53.44	90.72
3	BER	0.0066	4.79×10^{-4}	4.44×10^{-5}
	%	-	92.74	99.33
4	BER	0.0161	4.02×10^{-3}	1.19×10^{-3}
	%	-	75.03	92.61

A numerical representation of average BER result improvement is given in Table I. For different subcarrier bandwidths and modulation orders, BER results are shown and average percentage improvement of BER in dB scale with MRC algorithm are given for 1x2 and 1x3 SIMO systems compared to individual receiver modems' (1x1) BER at the same SNR level of 30 dB. In Table I, BPSK and QPSK symbol mapping for subcarrier bandwidth of 15.26 Hz are denoted as *Setting 1* and *2* respectively. Similarly, for subcarrier bandwidth of 7.63 Hz, BPSK and QPSK are given as *Setting 3* and *4* respectively.

IV. CONCLUSIONS

In this work, we presented a testbed and experimental evaluation for distributed SIMO systems. By utilizing software-defined underwater acoustic modems, ZP-OFDM signals are transmitted and received from three different receivers simultaneously. MRC processing is applied as 1x2 SIMO pairs and

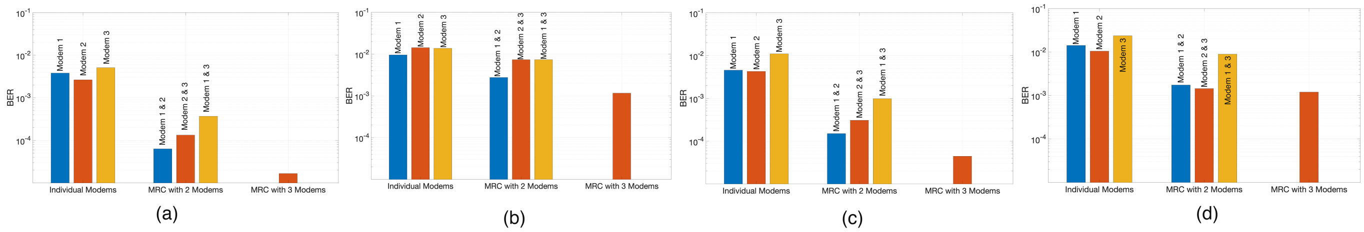

Fig. 12. For different ZP-OFDM waveforms of (a) 15.26 Hz subcarrier bandwidth with BPSK, and (b) QPSK and (c) 7.63 Hz subcarrier bandwidth with BPSK, and (d) QPSK modulations, BER results and comparisons for individual receivers, 1x2, and 1x3 SIMO systems evaluated through the experiments are shown.

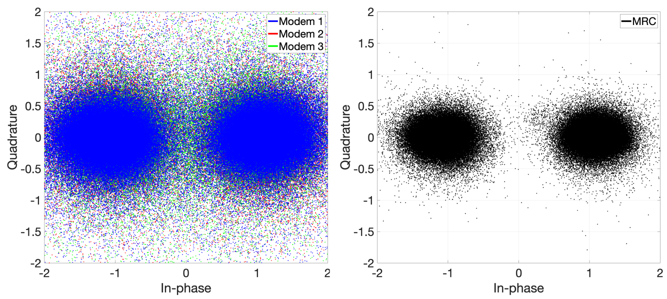

Fig. 13. Constellation graph for individual receivers (left) and output of the MRC for 1x3 SIMO system (right) is given for ZP-OFDM signaling with 15.26 Hz subcarrier bandwidth and BPSK modulation. Significant improvement for decreasing the spreading of bits is observed.

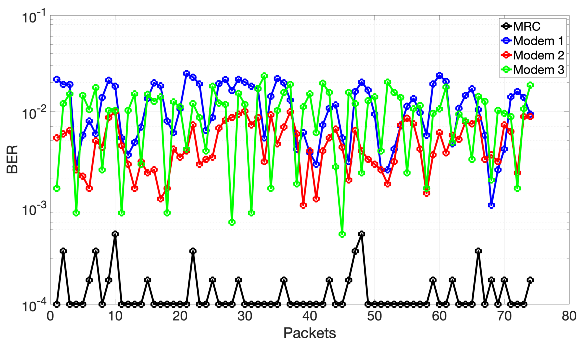

Fig. 14. BER distribution for each packet for individual receivers and output of the MRC for 1x3 SIMO system is given for ZP-OFDM signaling with 15.26 Hz subcarrier bandwidth and BPSK modulation.

1x3 SIMO system by using the utilized receiver modems. BER results are obtained for four different ZP-OFDM settings, where subcarrier bandwidth and modulation order are differentiated. Results show that our proposed distributed SIMO system, both for 1x2 and 1x3 settings, can outperform individual receiver modems, in terms of BER performance by 95.20% and 99.57%, respectively. It is concluded that significant performance improvements can be achieved using a distributed SIMO system incorporating MRC method.

Future research directions will include implementation of MRC for real-time processing. This implementation will be evaluated with a transmitter modem that is mobile, such as remotely operated vehicles (ROV) or unmanned underwater vehicles (UUV).

References

[1] T. Melodia, H. Kulhandjian, L. Kuo, and E. Demirors, "Advances in underwater acoustic networking," in *Mobile Ad Hoc Networking: Cutting Edge Directions*, 2nd ed., S. Basagni, M. Conti, S. Giordano, and I. Stojmenovic, Eds. Inc., Hoboken, NJ: John Wiley and Sons, 2013, pp. 804–852.

[2] L. Lanbo, Z. Shengli, and C. Jun-Hong, "Prospects and problems of wireless communication for underwater sensor networks," *Wireless Communications and Mobile Computing*, vol. 8, no. 8, pp. 977–994, 2008.

[3] E. Demirors, J. Shi, R. Guida and T. Melodia, "SEANet G2: A Toward a High-Data-Rate Software-Defined Underwater Acoustic Networking Platform," in *Proc. of ACM Intl. Conf. on Underwater Networks & Systems (WUWNet)*, Shanghai, China, October 2016.

[4] E. Demirors, J. Shi, A. Duong, N. Dave, R. Guida, B. Herrera, F. Pop, G. C. C. Casella, S. Tadayon, M. Rinaldi, S. Basagni, M. Stojanovic, and T. Melodia, "The SEANet Project: Toward a Programmable Internet of Underwater Things," in *Proc. of IEEE Underwater Communications Conf. And Workshop (UComms)*, Lerici, Italy, August 2018.

[5] S. Falleni, D. Unal, A. Neerman, K. Enhos, E. Demirors, S. Basagni, and T. Melodia, "Design, development, and testing of a smart buoy for underwater testbeds in shallow waters," in *Proceedings of IEEE/MTS Global OCEANS 2020*, Singapore–U.S. Gulf Coast, October 5–14 2020, pp. 1–7.

[6] B. Li, J. Huang, S. Zhou, K. Ball, M. Stojanovic, L. Freitag, and P. Willett, "Mimo-ofdm for high-rate underwater acoustic communications," *IEEE Journal of Oceanic Engineering*, vol. 34, no. 4, pp. 634–644, 2009.

[7] Y. Emre, V. Kandasamy, T. M. Duman, P. Hursky, and S. Roy, "Multiinput multioutput ofdm for shallow-water uwa communications," *The Journal of the Acoustical Society of America*, vol. 123, no. 5, pp. 3891–3891, 2008. [Online]. Available: https://doi.org/10.1121/1.2935839

[8] P. C. Carrascosa and M. Stojanovic, "Adaptive mimo detection of ofdm signals in an underwater acoustic channel," in *OCEANS 2008*, 2008, pp. 1–7.

[9] G. Sklivanitis, Y. Cao, S. N. Batalama, and W. Su, "Distributed mimo underwater systems: Receiver design and software-defined testbed implementation," in *2016 IEEE Global Communications Conference (GLOBECOM)*, 2016, pp. 1–7.

[10] D. Unal, S. Falleni, E. Demirors, K. Enhos, S. Basagni, and T. Melodia, "Software-defined underwater acoustic networking platform for underwater vehicles," in *2022 IEEE International Conference on Communications (ICC)*, 2022.

[11] A. Goldsmith, *Wireless Communications*. USA: Cambridge University Press, 2005.

[12] B. Li, S. Zhou, M. Stojanovic, L. Freitag, and P. Willett, "Multicarrier communication over underwater acoustic channels with nonuniform doppler shifts," *IEEE Journal of Oceanic Engineering*, vol. 33, no. 2, pp. 198–209, 2008.

[13] J. Barry, E. Lee, and D. Messerschmitt, *Digital Communication*. Springer US, 2004, no. 1. c. [Online]. Available: https://books.google.com.tr/books?id=hPx70ozDJlwC

[14] Z. Li and M. Stojanovic, "Multi-user multi-carrier underwater acoustic communications," in *Global Oceans 2020: Singapore – U.S. Gulf Coast*, 2020, pp. 1–4.